

STABILITY TEST OF 4 FT² TRIPLE-JUNCTION a-Si ALLOY PV PRODUCTION MODULES

X. DENG, M. IZU, K. L. NARASIMHAN AND S. R. OVSHINSKY
Energy Conversion Devices, Inc., 1675 West Maple Road, Troy, MI 48084

ABSTRACT

We report results of stability tests of 4 ft² triple-junction a-Si alloy photovoltaic (PV) modules. These modules were produced in ECD's 2 Megawatt (MW) continuous, roll-to-roll PV manufacturing line during the early stage of optimization. The stable module efficiency after 600 hours of 1 sun light soaking at approximately 50°C under load, is 8%. This is the highest stable efficiency for large area (≥ 4 ft²) a-Si alloy PV modules made in a production line.

INTRODUCTION

During the past 20 years, Energy Conversion Devices, Inc. (ECD), has significantly advanced the development of materials, device designs, and manufacturing processes required for the commercial acceptance of photovoltaic technology.¹⁻¹⁵ Among these advancements, ECD pioneered and continues development of a low cost, roll-to-roll continuous substrate a-Si alloy thin film solar cell manufacturing process to achieve the cost and efficiency goals necessary for the widespread growth of the photovoltaic market.

ECD has recently designed and constructed a 2 MW PV module manufacturing plant for Sovlux, ECD's Russian joint venture company with Kvant. This manufacturing line utilizes a proprietary continuous, roll-to-roll manufacturing process to produce triple-junction, two band-gap solar cells having a device configuration that has previously demonstrated 13.7% initial efficiency in small area cells.⁸ 4 ft² a-Si alloy PV modules have been produced in this manufacturing line using an optimized process. We have previously reported the progress and achievements made in this production line.¹⁶⁻¹⁷ In this paper we report the details of the module stability test and the process optimization toward achieving the highest stable efficiency.

MODULE MANUFACTURING PROCESS

In ECD's current 2 MW PV Manufacturing line, a-Si alloy solar cells are deposited in a continuous, roll-to-roll process on a 0.005 in. thick, 14 in. wide, 2500 ft. long web of stainless steel at a speed of 1 ft/min. Figure 1 illustrates the structure of the solar cells produced by this process.

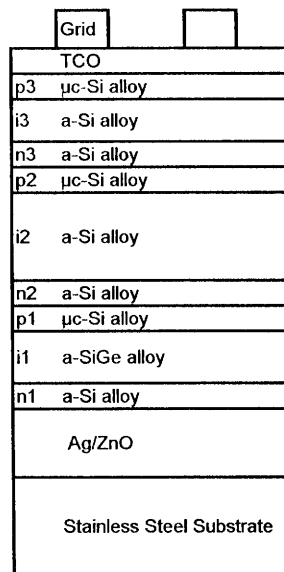


Figure 1 Structure of solar cells produced in ECD's triple-junction continuous roll-to-roll manufacturing line.

The deposition facility of the manufacturing line consists of four continuous roll-to-roll machines: i) a continuous roll-to-roll substrate washing machine; ii) a continuous roll-to-roll back-reflector machine that deposits a textured Ag/ZnO layers using DC magnetron sputtering; iii) a continuous roll-to-roll a-Si alloy rf PECVD deposition machine that produces, in a single pass, sequentially deposited thin films of doped and undoped amorphous silicon alloy semiconductors; and iv) a continuous roll-to-roll transparent conductor deposition machine that deposits a TCO layer on top of the solar cell using reactive evaporation.

In the continuous, roll-to-roll a-Si alloy deposition machine, triple-junction, two-bandgap a-Si/a-Si/a-SiGe solar cells with a bandgap profiled a-SiGe intrinsic layer in the bottom cell are deposited. Layers of n, i, and p are deposited in designated chambers that are separated by proprietary "gas gates". The "gas gates" utilize laminar gas flow through constant geometrical cross section conduits in a direction opposite to the diffusion gradient of the dopant gas concentrations. In this way, migration of dopants between chambers is essentially eliminated and gas mixtures in adjacent chambers are effectively isolated even though no actual physical impediment is present.

The module assembly process consists of the following procedures: i) cutting of TCO coated a-Si solar cell rolls into 16 in. long, 14 in. wide slabs; ii) quality assurance and quality control (QA/QC) for performance qualification of the production roll; iii) TCO scribing with screen printed etching paste; iv) short and shunt passivation; v) screen printing of Ag paste of grid pattern; and vi) final assembly which includes: cell cutting, interconnecting, module laminating, finishing, testing and packaging.

DETAILS OF LIGHT STABILITY TEST

We conducted light soaking tests to measure the stable efficiency of our modules. Philips metal halide light bulbs, powered by appropriate ballasts were used for light soaking. The light intensity is measured with a silicon detector covered with a heat filter so that its quantum efficiency is approximately the same as an a-Si alloy solar cell. The light intensity inside the module area is within 20% of 100 mW/cm², with the average at 100 mW/cm². The temperature of the module under light soaking was about 50°C to 60°C. The temperature was slightly higher at the center of the module where the light intensity is about 20% higher than 100 mW/cm². Each module was operated during light soaking with a load so that it was operating at its peak power point.

STABLE EFFICIENCY OPTIMIZATION

We first describe the experimental process to optimize the stable efficiency of solar cells in the manufacturing machine. In a typical experimental deposition run, we deposit different sections of solar cells using a series of different deposition conditions on the continuous web. Although the a-Si alloy deposition machine is 21 m long, we produce a different experimental deposition each 3 m to 6 m of web (corresponding to 10 min to 20 min of deposition time) by changing the deposition conditions of different chambers in a timely manner while the web moves.

In Table 1 we show the results of one experimental run with five different deposition conditions. The solar cell data for each sample are the averages of approximately 10 cells fabricated in a QA/QC sample. Sample 1 was deposited under the standard conditions developed in previous runs. The V_{oc} , J_{sc} , FF and η are 2.368 V, 6.33 mA/cm², 0.662 and 9.92%.

Table 1 J-V data in the initial and degraded states for 6 QA/QC samples made under different deposition conditions in an experimental run.

Sample Number	Deposition Condition	Light Soaking Time (h)	Voc (V)	Jsc (mA/cm ²)	FF (%)	Eff (%)	Drop in Eff
Sample1	Standard	0	2.368	6.33	0.662	9.92	
		150	2.277	6.13	0.582	8.12	18.2%
Sample2	Standard (30m from sample 1)	0	2.362	6.32	0.659	9.84	
		150	2.269	6.15	0.581	8.11	17.6%
Sample3	i1:13%less GeH4 i1:30%thicker i3:5% thinner	0	2.390	6.26	0.667	9.97	
		150	2.293	6.08	0.582	8.12	18.6%
Sample4	i2:10%thicker	0	2.365	6.36	0.663	9.97	
		150	2.274	6.20	0.580	8.17	18.0%
Sample5	i2:10%thinner i3:5%thinner	0	2.359	6.14	0.671	9.72	
		150	2.264	5.99	0.588	8.00	17.7%
Sample6	i2:25C higher Ts i2:5%thinner	0	2.323	6.35	0.661	9.74	
		150	2.243	6.24	0.588	8.23	15.5%

of running time, it was deposited 1.5 hours later. The solar cell data of Sample 2 in both the initial and degraded states are very similar to that of Sample 1, indicating excellent uniformity and consistency in different sections of the web and excellent reproducibility at different times in the deposition process.

Sample 3 in Table 1 was deposited under different conditions. Compared to the standard Sample 1 condition, the i1 layer was deposited with 13% less GeH₄/(GeH₄+Si₂H₆) in the gas mixture and 30% higher rf power, consequently the i1 layer has higher bandgap and is thicker. The i1 layer was defined previously in Figure 1. Although the i1 layer is about 30% thicker, the total current in the bottom cell is still less than Sample 1 due to the reduced Ge content, as we found out from the quantum efficiency (QE) curve of similar samples. Therefore, the i3 layer of Sample 3 is made with 5% less rf power so that about the same mismatch is maintained between the component cells and the overall FF of the triple cell can be approximately the same. The solar cell data of Sample 3 does show higher V_{oc}, lower current and about the same FF, as expected. The solar cell efficiency of Sample 3 in the degraded state, is the same as Sample 1 and Sample 2.

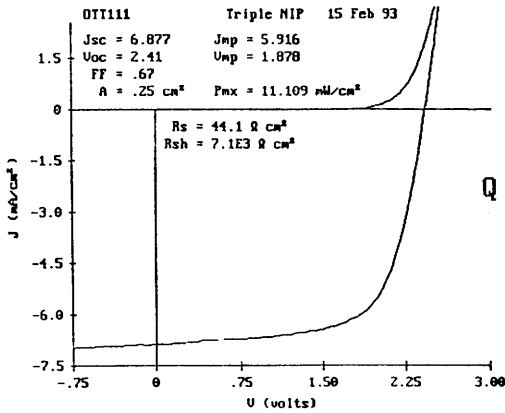
A 10% thicker i2 layer in Sample 4 does not result in any sizable change in V_{oc}, J_{sc} and FF compared to Sample 1 since in both samples the solar cells are limited by the top component cell. Sample 5 shows lower J_{sc} and higher FF when i2 and i3 were both made thinner thus more light is absorbed by the bottom cell. The increased mismatch results in a higher overall FF.

In Sample 6, the i2 layer was made at 25°C higher substrate temperature than the standard. Since it has a lower bandgap due to the increased temperature, it is made with 5% less power to get approximately the same J_{sc} for the middle cell, so that the same matching is maintained between the component cells. Although the initial efficiency is relatively low due to the reduced V_{oc}, the efficiency in the degraded state is the highest among the six samples. This is due to the improved stability of the i2 layer when it is deposited at relatively higher temperature.

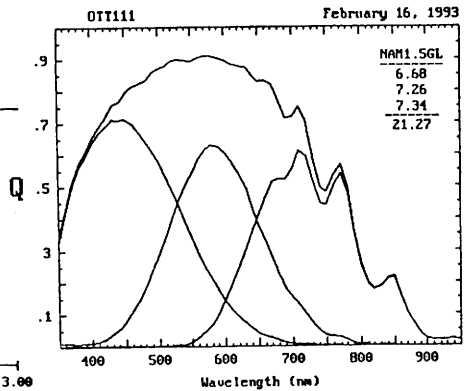
After process optimization, we produced triple-junction solar cells with 11.1% initial active area conversion efficiency. This is the highest initial active-area efficiency reported for any a-Si alloy solar cell made in a production machine. The J-V characteristics and quantum efficiency curves of the solar cell are shown in Figure 2 (a) and 2 (b). This cell was deposited in a 2500 ft. long production run.

To study the light stability behavior of samples made under different conditions, we light soak these samples under 1 sun illumination at approximately 40°C to 50 °C under open circuit condition for 150 hours. After degradation, Sample 1 shows V_{oc}, J_{sc}, FF and η of 2.277 V, 6.13 mA/cm², 0.582 and 8.12% with a drop in η of 18.2%.

Sample 2 in Table 1 is deposited under identical condition but collected 30 m farther down the web than Sample 1. In terms



(a) J-V curve



(b) Quantum efficiency curve

Figure 2 11.1% efficient solar cell deposited in a 2500 ft production run.

We assembled 4 ft² modules with this solar cell using the steps described above. Figure 3 is the I-V curve of a 4 ft² module (ECD030) measured by the National Renewable Energy Laboratory (NREL). The initial aperture area efficiency is 9.5%, the highest efficiency for 4 ft² a-Si alloy PV module produced in a production line.

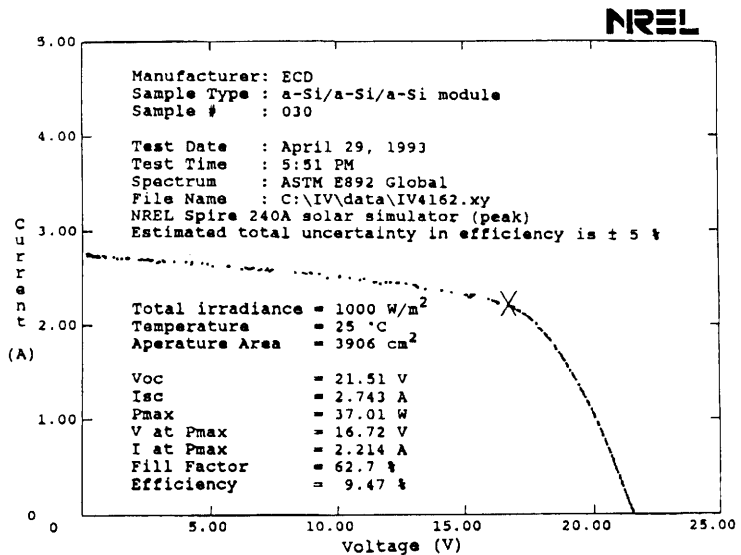


Figure 3 I-V curve of an ECD 4 ft² production module measured by NREL, showing 9.5% initial module efficiency.

We have light soaked these 4 ft² modules under 1 sun intensity at approximately 50 to 60°C under load. The module efficiency after 600 hours of light soaking is 8%, as shown in Figure 4. This is the highest reported stable efficiency for a large area (4 ft²) a-Si alloy PV production module. It was achieved during the initial optimization of ECD's 2 MW continuous roll-to-roll

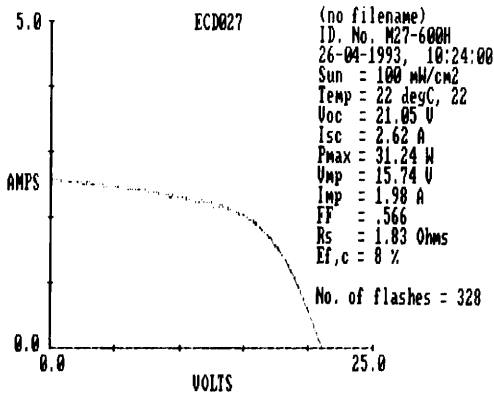


Figure 4: I-V curve of an ECD 4 ft² production module after 600 hours of light soaking, showing 8% stable efficiency.

manufacturing line, which is capable of producing 10% stabilized efficiency modules. In Table 2, we list the initial and stabilized performance data of ECD's 4 ft² production modules measured at ECD and NREL. We have further light soaked one 4 ft² module up to 2380 hours. In Figure 5, we show the semilog curves of V_{oc}, J_{sc}, FF and η of two modules as a function of light soaking time. As can be seen from the curve, the degradation happens mostly during the first 100 hours of light soaking.

At this meeting, a breakthrough 10.2% stabilized efficiency¹⁸ has been announced for 1 ft² a-Si alloy modules, which were made in a batch deposition system. Through the years, we have always been able to institute in a continuous web process what has been achieved in batch deposition process.

SUMMARY

4 ft² triple-junction a-Si alloy PV modules were produced in ECD's 2 MW continuous, roll-to-roll manufacturing line. These modules show initial aperture area efficiency of 9.5%. After light soaking under 1 sun illumination at approximately 50°C-60°C under load for 600 hours, the module efficiency has stabilized at 8%. This is the highest stable efficiency for a-Si alloy PV modules produced in a manufacturing line.

ACKNOWLEDGMENTS

The authors would like to thank: S. Guha, J. Yang, H. Fritzsche, A. Krisko, H.C. Ovshinsky, K. Whelan, R. Young and other ECD project team members for discussions and collaborations. This work was supported by DOE/NREL PVMat-2A program under subcontract number ZM-2-1104-7.

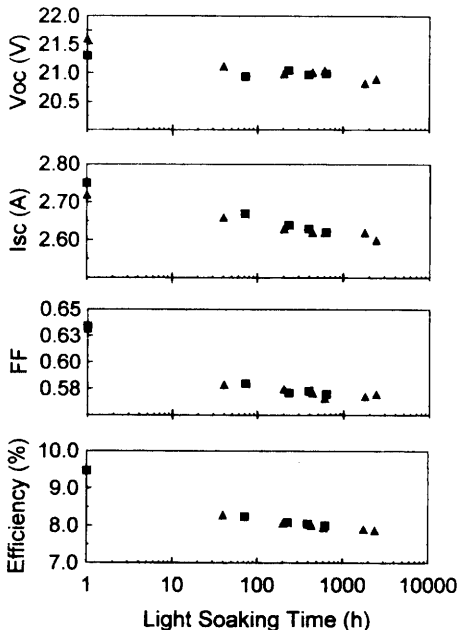


Figure 5: Semilog plots of V_{oc}, I_{sc}, FF and Eff of two 4 ft² modules as a function of light-soaking time.

Table 2 Module performance data of ECD's 4 ft2 modules in the initial and stable states measured at ECD and NREL.

Module Number	Light Soaking Time (hours)	Voc (V)	Isc (A)	FF	Pmax (W)	Area (cm ²)	Efficiency (%)	Measurement Lab
#23	Initial	21.62	2.68	0.628	36.39	3907	9.31	ECD
	Initial	21.56	2.72	0.63	36.96	3906	9.46	NREL
#27	Initial	21.6	2.72	0.632	37.18	3923	9.48	ECD
	2380	20.9	2.60	0.57	30.93	3923	7.9	ECD
	2380	21.0	2.56	0.566	30.42	3903	7.8	ECD
	2380	20.87	2.534	0.57	30.17	3903	7.73	NREL
#28	Initial	21.3	2.75	0.634	37.15	3923	9.47	ECD
	625	20.99	2.62	0.57	31.38	3923	8.00	ECD
	625	20.87	2.57	0.571	30.64	3906	7.84	NREL
#30	Initial	21.61	2.68	0.63	36.57	3907	9.36	ECD
	Initial	21.51	2.74	0.627	37.01	3906	9.47	NREL

REFERENCES

1. S. R. Ovshinsky, *New Scientist*, November 30, 1978.
2. S. R. Ovshinsky, *J. of Non-Cryst. Solids*, 32, 17 (1979).
3. See, for example, papers in book series *Disordered Materials*, published by Institute for Amorphous Study.
4. M. Izu and S. R. Ovshinsky, *SPIE Proc.* 407, 42 (1983).
5. M. Izu and S. R. Ovshinsky, *Thin Solid Films* 119 55 (1984).
6. H. Morimoto and M. Izu, *JARECT 16* (1984); *Amorphous Semiconductor Technology & Devices*, North Holland Publishing Company, Edited by Y. Hamakawa, 212 (1984).
7. S. R. Ovshinsky, *Proc. International PVSEC-1*, 577 (1988).
8. J. Yang, R. Ross, T. Glatfelter, R. Mohr, G. Hammond, C. Bernotaitis, E. Chen, J. Burdick, M. Hopson and S. Guha, *Proc. 20th IEEE PV. Spec. Conf.* 241 (1988).
9. J. Yang, R. Ross, R. Mohr and J. P. Fournier, *Proc. MRS Symp. Vol. 95*, 517 (1987).
10. P. Nath and M. Izu, *Proc. 18th IEEE PV Spec. Conf.*, 939 (1985).
11. P. Nath, K. Hoffman, J. Call, C. Vogeli, M. Izu and S. R. Ovshinsky, *Proc. of the 3rd International Photovoltaic Science and Engineering Conf.*, Tokyo, Japan, 395 (1987).
12. P. Nath, K. Hoffman, C. Vogeli and S. R. Ovshinsky, *Appl. Phys. Lett.* 53 (11), 986 (1988).
13. P. Nath, K. Hoffman and S. R. Ovshinsky, *4th International P.V. Science and Engineering Conf.*, Sydney, Australia, (1989).
14. S. Guha, *Proc. MRS Spring Meeting, San Diego, April* (1989).
15. J. Yang, R. Ross, T. Glatfelter, R. Mohr and S. Guha, *MRS Proc.* 149, 435 (1989).
16. M. Izu, X. Deng, A. Krisko, K. Whelan, R. Young, H.C. Ovshinsky, K.L. Narasimhan and S.R. Ovshinsky, *proc. 23rd IEEE PV Spec. Conf.*, 919 (1993).
17. M. Izu, S.R. Ovshinsky, X. Deng, A. Krisko, H.C. Ovshinsky, K.L. Narasimhan, and R. Young, *Proc. of 12th NREL PV Program Review Meeting, October, 1993*.
18. S. Guha, J. Yang, A. Banerjee, T. Glatfelter, K. Hoffman, S. R. Ovshinsky, M. Izu, H.C. Ovshinsky, and X. Deng, *Proc. MRS spring meeting 1994, this volume*.